

Article

Life Cycle Assessment as a Decision-Making Tool for Photochemical Treatment of Iprodione Fungicide from Wastewater

Kubra Dogan ¹, Burcin Atilgan Turkmen ², Idil Arslan-Alaton ^{1,*}  and Fatos Germirli Babuna ¹ 

¹ Environmental Engineering Department, Civil Engineering Faculty, Istanbul Technical University, 34469 Istanbul, Turkey; kubradgn46@gmail.com (K.D.); germirliba@itu.edu.tr (F.G.B.)

² Chemical Engineering Department, Engineering Faculty, Bilecik Seyh Edebali University, 11230 Bilecik, Turkey; burcin.atilganturkmen@bilecik.edu.tr

* Correspondence: arslanid@itu.edu.tr

Abstract: Water contamination with various micropollutants is a serious environmental concern since this group of chemicals cannot always be removed efficiently with advanced treatment methods. Therefore, alternative chemical- and energy-intensive oxidation processes have been proposed for the removal of refractory and/or toxic chemicals. However, similar treatment performances might result in different environmental impacts. Environmental impacts can be determined by adopting a life cycle assessment methodology. In this context, lab-scale experimental data related to 100% iprodione (a hydantoin fungicide/nematicide selected as the model micropollutant at a concentration of 2 mg/L) removal from simulated tertiary treated urban wastewater (dissolved organic carbon content = 10 mg/L) with UV-C-activated persulfate treatment were studied in terms of environmental impacts generated during photochemical treatment through the application of a life cycle assessment procedure. Standard guidelines were followed in this procedure. Iprodione removal was achieved at varying persulfate concentrations and UV-C doses; however, an “optimum” treatment condition (0.03 mM persulfate, 0.5 W/L UV-C) was experimentally established for kinetically acceptable, 100% iprodione removal in distilled water and adopted to treat iprodione in simulated tertiary treated wastewater (total dissolved organic carbon of iprodione + tertiary wastewater = 11.2 mg/L). The study findings indicated that energy input was the major contributor to all the environmental impact categories, namely global warming, abiotic depletion (fossil and elements), acidification, eutrophication, freshwater aquatic ecotoxicity, human toxicity, ozone depletion, photochemical ozone creation, and terrestrial ecotoxicity potentials. According to the life cycle assessment results, a concentration of 21.42 mg/L persulfate and an electrical energy input of 1.787 kWh/m³ (Wh/L) UV-C light yielded the lowest undesired environmental impacts among the examined photochemical treatment conditions.



Citation: Dogan, K.; Turkmen, B.A.; Arslan-Alaton, I.; Germirli Babuna, F. Life Cycle Assessment as a Decision-Making Tool for Photochemical Treatment of Iprodione Fungicide from Wastewater. *Water* **2024**, *16*, 1183. <https://doi.org/10.3390/w16081183>

Academic Editor: Jingguo Li

Received: 2 October 2023

Revised: 1 November 2023

Accepted: 18 April 2024

Published: 21 April 2024

Keywords: environmental impacts; life cycle assessment (LCA); advanced oxidation processes (AOPs); photochemical treatment of micropollutants; fungicide; iprodione; tertiary treated urban wastewater



Copyright: © 2024 by the authors. Licensee MDPI, Basel, Switzerland. This article is an open access article distributed under the terms and conditions of the Creative Commons Attribution (CC BY) license (<https://creativecommons.org/licenses/by/4.0/>).

1. Introduction

Due to serious water pollution problems arising from intensive agricultural activities, it is becoming mandatory to examine the environmental impact of wastewater treatment systems to properly protect and manage water resources. The recommendation of a proper wastewater treatment method is typically based on its performance, which is commonly measured as an absolute or relative removal efficiency/rate. However, such a limited assessment will probably fail since a wide range of environmental impacts are easily overlooked. A combined assessment of economic and environmental impacts is particularly critical when it comes to decision-making in developing countries where the application

of high-energy, expensive, and advanced treatment methods is very hard to implement and questionable.

Treatment alternatives applicable to municipal wastewaters are evaluated based on conventional polluting parameters such as the chemical oxygen demand (COD) without addressing micropollutants. It is a known fact that quite an array of micropollutants are not removed during conventional municipal wastewater treatment [1–4]. As a result, since they are mixed with the water resource, the micropollutants, in further scarce concentrations, continue to pose a threat to the water ecosystem in which they are introduced. Depending on the use of the mentioned water body, another treatment might be required to remove these micropollutants when water is withdrawn from it.

One of the most improved tools for objectively obtaining the environmental impacts of products [5,6], processes [7–9], and services is the life cycle assessment (LCA) methodology. The environmental impacts generated during different life stages of treatment systems have been investigated in the literature, such as the operation [10,11] and construction [12] of municipal water treatment work, the operation of a domestic wastewater treatment facility [13], and the operation and maintenance of two alternative industrial water treatment systems [14]. Addressing sustainability issues along with preliminary treatability evaluations is of importance for soundly defining the treatment alternatives and operating conditions of treatment systems. A study combining the treatability results with the environmental impacts arising from the treatment alternatives for a segregated textile dyebath discharge can be considered a pioneering effort [15]. The mentioned study addresses a sound roadmap to reach the most environmentally favorable treatment conditions [15].

As indicated earlier, wastewater treatment issues are strongly linked to micropollutants released into the aquatic environment, causing serious management concerns. So far, several studies have already investigated the outcome, impact, and treatability of various micropollutants originating from industrial, household, and agricultural activities [16]. For instance, the micropollutant iprodione (3-(3,5-Dichlorophenyl)-2,4-dioxo-*N*-(propan-2-yl)imidazolidine-1-carboxamide) is a hydantoin fungicide used on crops to fight various fungal plant diseases. It has been applied to a variety of crops, such as fruits, vegetables, ornamental trees, and lawns, as a contact biocide that inhibits the germination of fungal spores and the growth of fungal mycelium [17]. More recently, iprodione was also used to kill nematodes and filed for patent protection for that purpose [17]. Although its approval in the EU market was not renewed in 2017 [18] and the product was banned later in 2019 [19], since there was no alternative or replacement product recommended for this fungicide, its use in agricultural activities continued for a while in some countries, such as Turkey, that had used the fungicide intensively [20].

More recently, photochemical advanced oxidation processes (AOPs) have been applied to remove toxic and/or recalcitrant micropollutants found in water and wastewater, with promising results [21,22]. AOPs most often combine high-energy short ultra-violet (UV-C) light with common oxidants, including ozone or the peroxides hydrogen peroxide, peroxydisulfate, or percarbonate, to produce the reactive oxidizing agents hydroxide (HO•), sulfate (SO₄•⁻), and carbonate (CO₃•⁻) radicals, respectively [23,24]. Free radicals are known to react with organic (micro)pollutants a million-to-billion times faster than strong oxidants such as chlorine dioxide or ozone [25,26].

In persulfate (PS)-based AOPs, reactive oxygen species are generated upon activation of persulfates (mostly two precursor salts, namely peroxy disulfate and peroxy monosulfate) by UV-C light, metal oxides, transition metal ions, and zero-valent metals, as well as sonolytic and radiolytic activation [21,23,24]. PS activation involves O–O bond-breakage (bond distance = 1.497 Å; bond energy = 140 kJ/mol), which is similar to the more conventional peroxide H₂O₂ [22,23]. Among the variety of PS activation methods available, UV-C activation of PS is the most efficient and direct way to form SO₄•⁻, wherein one mole of PS undergoes UV-C photolysis at λ = 254 nm and is cleaved into two moles of SO₄•⁻ through the following reaction [24]:



The highest quantum yield of the above reaction in neutral solution is unity [24].

As with many other fungicides, iprodione is chemically, photochemically, and biochemically very stable and has long-term negative effects on the environment as well as human health [16]. In fact, an appreciable fraction of the AOP literature has focused on pesticide treatment. However, only limited information is currently available describing the photochemical degradation of iprodione [27–30]. In these few studies, dechlorination has been reported as a primary stage of iprodione degradation, followed by hydroxyl group replacement [27,28]. Only a few papers have reported the removal of iprodione using UV-C light and its combination with hydrogen peroxide from an aqueous solution [20,27–30]. Moreover, there is no study available in the scientific literature dealing with the environmental impacts of these rather energy-intensive, chemical-consuming treatment processes. Considering the above-mentioned gaps, in the present work, the UV-C/PS (the peroxide used in this work is sodium peroxydisulfate, PS) photochemical treatment process was applied under previously optimized PS concentration, pH, and UV-C dose to completely remove the model micropollutant iprodione (2 mg/L) from synthetic, tertiary treated municipal wastewater (overall DOC of the synthetic wastewater + DOC of the 2 mg/L iprodione solution = 11.2 mg/L) to examine its environmental impacts. These were assessed in more detail using the LCA methodology. This study focused on identifying the most sustainable energy and chemical management options for the treatment of the selected model micropollutants and the photochemical treatment process (UV-C/PS) at the lab scale.

2. Materials and Methods

UV-C/PS treatment of iprodione was carried out in synthetic wastewater samples mimicking real, tertiary treated urban wastewater. Tertiary treated urban wastewater (TWW) was prepared to represent wastewater taken from the effluent of a typical municipal wastewater treatment plant practicing tertiary biological treatment (combined biological C, N, and P removal). All chemicals and reagents used in this study were purchased from Sigma-Aldrich® (Merck, Istanbul, Turkey) and were of analytical grade. The composition of the TWW sample was composed of different organic and inorganic components: $(\text{NH}_4)_2\text{SO}_4$ (12 mg/L), tryptone (50 mg/L), meat extract (50 mg/L), yeast extract (7.5 mg/L), urea (7.5 mg/L), K_2HPO_4 (10 mg/L), $\text{CaCl}_2 \cdot 2\text{H}_2\text{O}$ (1 mg/L), and $\text{MgSO}_4 \cdot 7\text{H}_2\text{O}$ (1 mg/L) [20]. In addition to the above-mentioned chemicals, 4 mg/L of humic acid was also added to the reaction solution as an organic compound, which rendered the TWW composition more complex and typical for urban effluent. Urban wastewater generally contains a mixture of industrial wastewater, domestic wastewater, and run-off rainwater [20]. The pH of the TWW was around 6.4–6.8, and it was 5-fold diluted with distilled water (DW) to obtain a final DOC content of 10 mg/L, which is a typical DOC for tertiary treated effluent TWW. A more detailed preparation procedure for the TWW, as well as other details about its environmental characteristics, can be found in [20,30]. Before each experimental run, iprodione was spiked into either DW or TWW, depending on the experimental concept. All treatability experiments were conducted in a stainless-steel UV chamber (Luzchem Research Inc., Ottawa, Canada) equipped with ten short-UV (UV-C) fluorescent lamps, a magnetic stirring unit, and a cooling air fan to keep the temperature stable. A 500 mL-capacity, three-neck quartz flask (Yuwinsil Scientific Technology, Noida, India) was used as the photoreactor, and the introduced UV-C light flux was measured with a lux-meter incorporated in the reaction chamber and calculated as 0.5 W/L. More details of the experimental set-up can be found elsewhere [20,30].

In the photochemical treatability and optimization experiments that can be found in detail in [20,30], a range of sodium peroxydisulfate ($\text{Na}_2\text{S}_2\text{O}_8$; called PS) concentrations (0–1 mM) and pH values (3–11) at different levels of electrical energy input (applied UV-C dose) were used. Table 1 outlines the conditions set for various experimental runs. In this work, these optimum photochemical treatment conditions were further assessed in terms of their environmental impacts to establish the most sustainable treatment strategy for this micropollutant in TWW.

Table 1. Experimental conditions yielding 100% iprodione removal from TWW (iprodione concentration = 2 mg/L; overall DOC (iprodione + TWW) = 11.2 mg/L; original pH = 6.8).

Run	PS Concentration (mg/L)	Electrical Energy Consumption (kWh/m ³)
1	7.14	2.680
2	14.28	2.233
3	21.42	1.787

Some control experiments (PS only, UV-C only, aeration and mixing only, etc.) were also conducted with the TWW sample. All experimental results, data analyses, together with their respective kinetic calculations, were published elsewhere [20,30].

The LCA procedure was used to carry out an environmental impact assessment for each category based on the UV-C/PS treatment variables of iprodione using GaBi v7.3 software [31] and the Ecoinvent database [32] with the CML 2001 impact assessment method [33] on the basis of ISO 14040/14044 [34,35]. Hence, the iterative stages of goal and scope definition, inventory analysis, impact assessment, and interpretation are followed as defined by ISO 14040/14044. The purpose, scope, system boundaries, and functional unit for the system were defined during the goal and scope definition step. The raw material and energy components that entered the system for the life cycle inventory analysis, as well as the product and other components that left the system, were calculated in the inventory analysis step by associating them with the functional unit. The next step involved calculating environmental impact categories for each system component based on the life cycle impact assessment, and the final step involved interpreting the findings. The studied environmental impact categories were as follows: global warming potential (GWP), abiotic depletion potential (ADP fossil and elements), acidification potential (AP), eutrophication potential (EP), freshwater aquatic ecotoxicity (FAETP), human toxicity potential (HTP), ozone depletion potential (ODP), photochemical ozone creation potential (POCP), and terrestrial ecotoxicity potential (TETP). The functional unit was “1 m³ of treated wastewater”. Therefore, environmental impacts are presented on the basis of this functional unit.

The system boundaries set for the study are illustrated in Figure 1. As can be seen from the figure, the degradation of iprodione in a TWW sample is considered. Raw materials and energy input for the production of PS, together with the energy requirement for treatment, are covered. Waste due to treatment is not generated in this kind of photochemical process. The spent PS containers were collected by the supplier. Transportation of PS to the treatment site was also taken into account in this study.

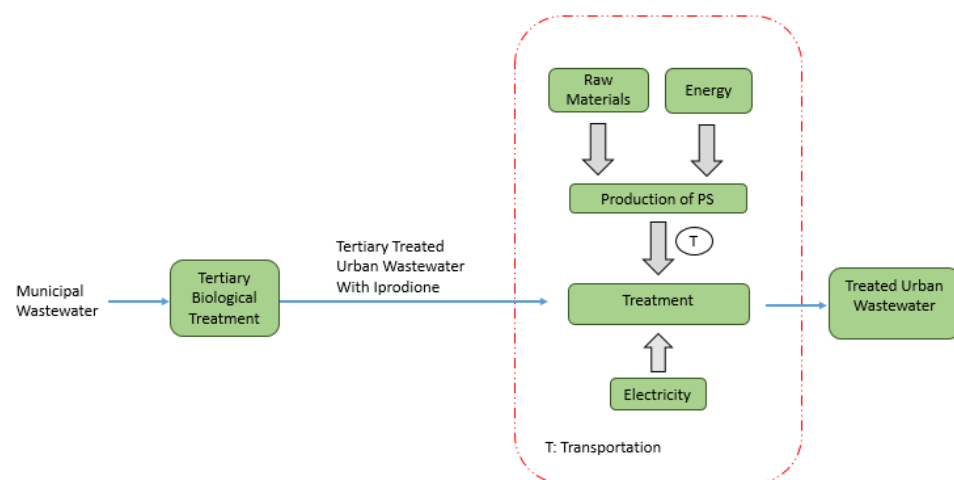


Figure 1. System boundaries established for iprodione removal from TWW.

The company that supplied the reagents is located in China. Therefore, 18,625 km of sea and 19 km of highway distance were considered for transportation. The highway transportation took place in trucks using diesel fuel.

Energy was taken from the Turkish electrical grid. For this purpose, a model was generated from the Ecoinvent database [32] by using the following percentages: hard coal (22%), natural gas (19%), lignite (15%), hydropower (29%), and other sources obtained from the Electricity Generation and Transmission Statistics of Turkey [36].

3. Results and Discussion

In the first stage of this experimental study, the UV-C/PS treatment of iprodione was optimized in terms of PS concentration, pH, and applied UV-C dose [20,30]. The PS concentration resulting in a kinetically superior iprodione removal rate and efficiency was established as 0.03 mM, the natural and working pH of DW/TWW was 6.2/6.8, and the treatment time was 120 min in total with UV-C radiation at 0.5 W/L. No pH adjustment was performed in the reaction solutions for the below-given experimental runs prior to photochemical treatment, and in this way, the pH was kept at a near-neutral value.

Figure 2 presents iprodione (initial concentration = 2 mg/L) abatements as a function of the applied UV-C dose (shown in Wh/L units) for the following experiments:

- (i) UV-C-only (0 mM PS) and UV-C/PS photochemical treatments of iprodione in DW (DOC of iprodione = 1.2 mg/L)
- (ii) UV-C-only (0 mM PS) and UV-C/PS photochemical treatments of iprodione in TWW (DOC of TWW = 10 mg/L; total DOC = 11.2 mg/L).

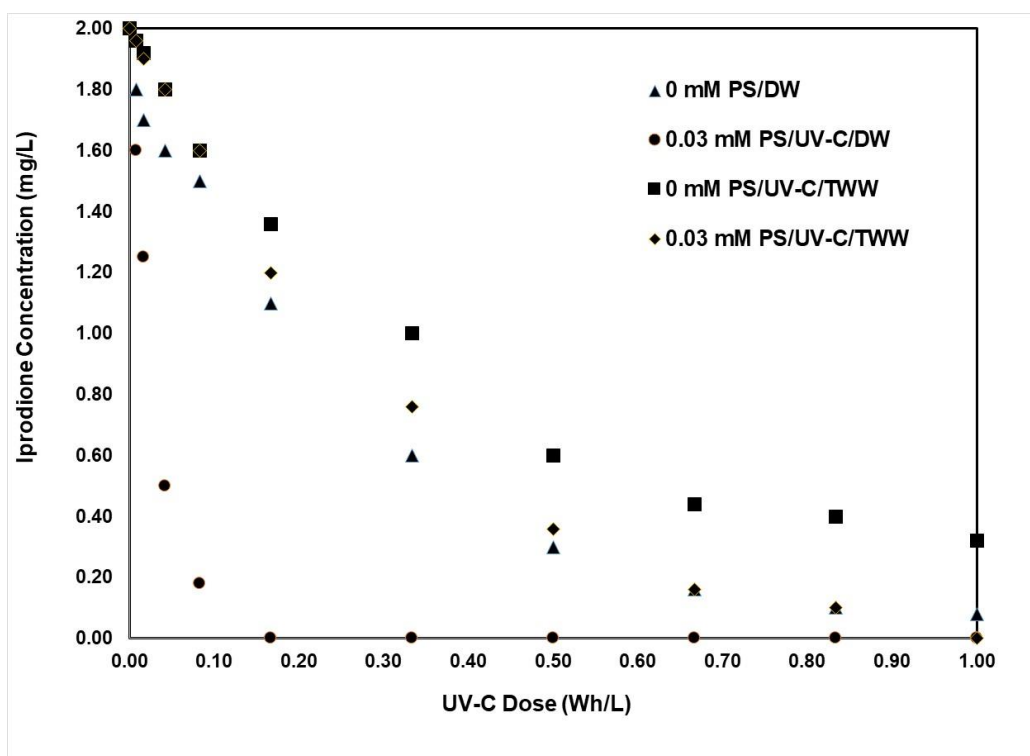


Figure 2. Iprodione (2 mg/L) abatements as a function of the applied UV-C dose (in Wh/L) for UV-C only (0 mM PS) and UV-C/PS (0.03 mM PS) treatments in DW (DOC of DW < 1 mg/L) and TWW (DOC of TWW = 10 mg/L; total DOC of TWW + Iprodione = 11.2 mg/L). The optimized PS concentration was selected as 0.03 mM, the natural pH of DW/TWW was 6.2–6.8, and the photochemical treatment time was 120 min in total.

From Figure 2 it is evident that the PS activation with UV-C light in the UV-C/PS treatment combination exhibits a strong synergy to remove the fungicide iprodione promptly

as compared to UV-C photolysis only (0 mM PS; the control experiment) acting as an AOP and hence producing reactive oxidant species. It is also apparent from Figure 2 that the wastewater ingredients (the high DOC content and presence of organic/inorganic ions, etc.) inhibit iprodione degradation, acting as free radical scavengers. The synergy between UV-C and PS functioning together as an AOP to produce the active oxidants (free radicals) HO^\bullet and $\text{SO}_4^{\bullet-}$ is needed for fast and complete iprodione removal. In fact, previous work has already demonstrated that organic pollutant removal in complex matrices like water and wastewater is negatively affected by the presence of their natural ingredients [37–45].

In particular, inorganic ions such as chloride could attack sulfate radicals and form chloride radicals, which would react more selectively, and hence more slowly, with the target pollutant and its metabolites, as shown in reaction Equation (1) [37,41,42].



In a similar manner, iprodione removals would be seriously halted during UV-C/PS treatment in the presence of organic matter, speculatively due to bulk phase competition reactions between iprodione and dissolved organics (present in the reaction solution) for sulfate radicals (similar to reaction Equation (1)). Among the organic compounds found in water and wastewater, carboxylic acids and natural organic matter (humic or fulvic acids) are known as strong free radical scavengers beyond a critical concentration [37–39,41,42].

In order to determine the most sustainable treatment alternative, the experimental conditions resulting in 100% iprodione removal from TWW (as presented in Table 1) are investigated in terms of their environmental impacts. Raw materials and energy used to produce PS, transportation of PS to the treatment site, and electricity required to generate UV-C are considered while revealing the environmental impacts using the LCA. The results of the LCA study are outlined in Table 2, and a comparative assessment of the environmental impacts of runs is illustrated in Figure 3.

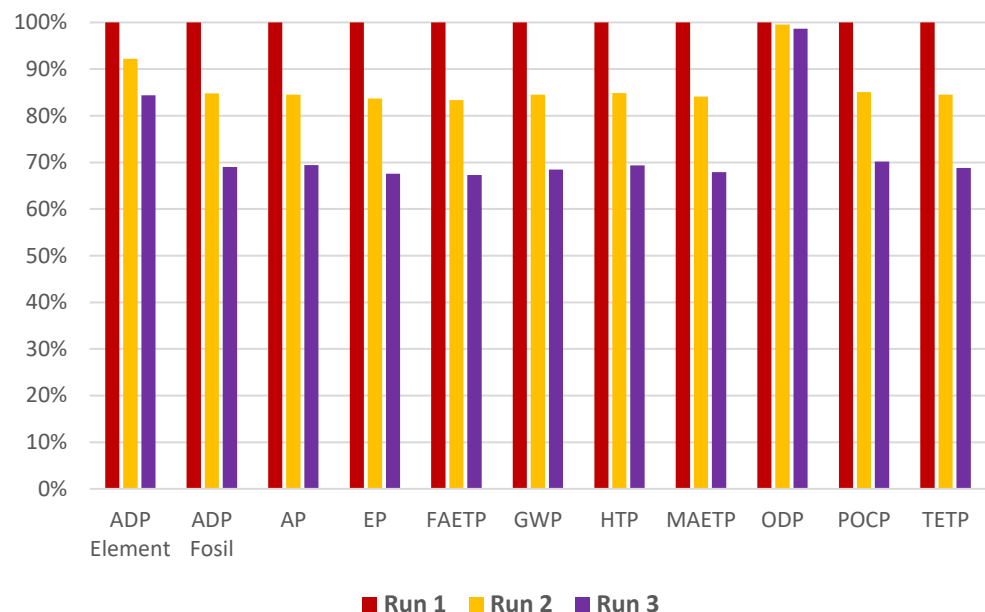


Figure 3. Comparative evaluation of the environmental impacts of iprodione removal from TWW.

As evident from Figure 3, Run 3 with 21.42 mg/L PS and a 1.787 kWh/m³ (Wh/L) UV-C electrical energy input gave the lowest undesired environmental impacts among the examined photochemical treatment options when energy is obtained from a grid electricity mix. For ODP, similar levels of environmental impacts are obtained for all the runs. Approximately 30% reductions can be achieved by applying the conditions of Run 3 instead of Run 1, apart from ODP and ADP elements. Run 3 (Iprodione 3) is observed to decrease ADP elements by around 15% in comparison with Run 1 (Iprodione 1).

Table 2. Environmental impacts of iprodione removal from TWW.

Impact Category	Experimental Runs		
	Run 1	Run 2	Run 3
ADP Elements (kg Sb-Equiv.)	2.31E−06	2.13E−06	1.95E−06
ADP Fossil (MJ)	1.71E+01	1.45E+01	1.18E+01
AP (kg SO ₂ -Equiv.)	1.08E−02	9.13E−03	7.50E−03
EP (kg PO ₄ -Equiv.)	6.69E−03	5.60E−03	4.52E−03
FAETP (kg DCB-Equiv.)	1.56E+00	1.30E+00	1.05E+00
GWP (kg CO ₂ -Equiv.)	1.68E+00	1.42E+00	1.15E+00
HTP (kg DCB-Equiv.)	1.05E+00	8.91E−01	7.28E−01
MAETP (kg DCB-Equiv.)	3.77E+03	3.17E+03	2.56E+03
ODP (kg R11-Equiv.)	2.22E−08	2.21E−08	2.19E−08
POCP (kg C ₂ H ₄ -Equiv.)	5.43E−04	4.62E−04	3.81E−04
TETP (kg DCB-Equiv.)	1.23E−02	1.04E−02	8.46E−03

For all experimental runs (Runs 1, 2, and 3), the impact of ADP elements is generated due to the depletion of nonrenewable elements, mainly copper. ADP fossil, on the other hand, is obtained for all the runs due to the consumption of hard coal, lignite, and natural gas.

The contribution of electricity input, PS production, and transportation of the chemical to the total impacts is presented in Figure 4. For Run 1, Run 2, and Run 3 experiments, most of the impacts, including ADP fossil, AP, EP, FAETP, GWP, HTP, MAEPT, POCP, and TETP, are mainly caused by electricity consumption, accounting for more than 95% of the total effects. The high proportion of coal and natural gas used in Turkey’s electricity mix is the primary cause of the ADP fossil element. The use of non-renewable elements, like copper, contributed significantly to the ADP element values across all sets of experiments. Atmospheric emissions of SO₂ and NO are mainly responsible for the AP of all the runs. Phosphate emissions in the water generate EP for all experimental runs. FAETP is generated mainly because of copper, nickel, and beryllium discharges in the water. Atmospheric emissions of CO₂ are the leading cause of GWP for all the investigated runs. HTP is generated due mainly to selenium emissions in water. Beryllium emissions in the water can be stated as the major cause of MAETP. Halon and tetrachloromethane emissions in the atmosphere are generating ODP for all the runs. SO₂ and nitrous oxide emissions in the atmosphere result in POCP. TETP is created mainly due to hexavalent chromium-Cr(+VI) emissions in the soil for all the runs under assessment.

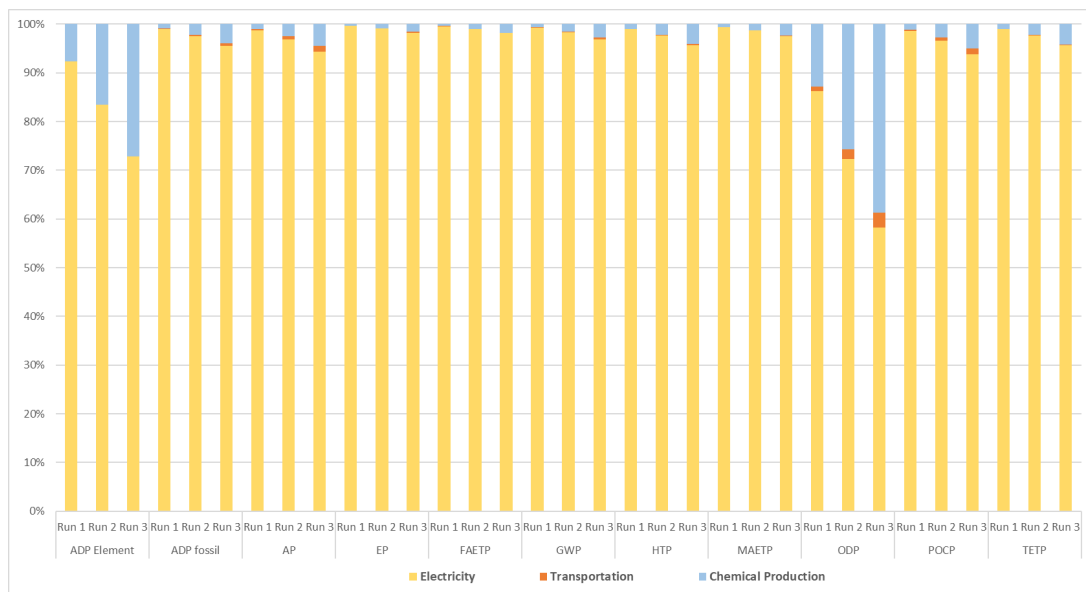


Figure 4. Contribution of various factors to the selected environmental impact categories.

The above findings indicated that energy input is the most important contributor to the environmental impact categories. After energy input, chemical production follows for ADP elements and then ODP. Furthermore, transportation has an insignificant effect on the environmental impact categories.

Since energy requirements play a significant role in all the investigated environmental impact categories, scenarios are established by changing the source of energy. For this purpose, the impacts arising from grid electricity, solar energy, and wind energy are compared as given in Figure 5 (normalized for Run 1—grid electricity as an energy source).

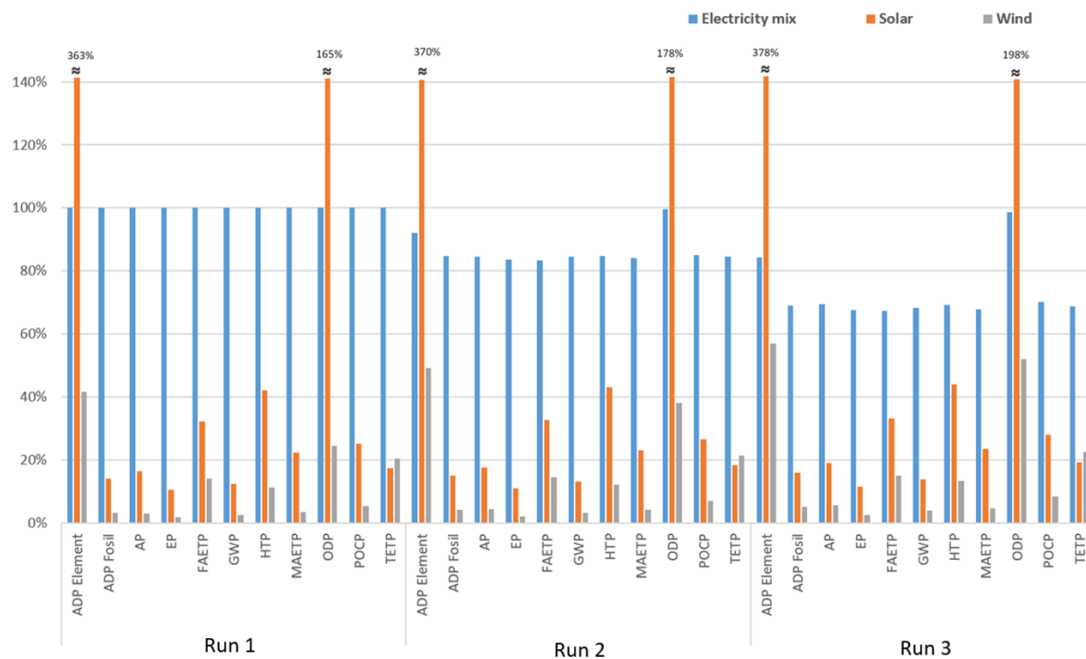


Figure 5. Comparative evaluation of energy support from various sources (normalized for Run 1—grid electricity).

According to the results illustrated in Figure 5, in comparison with Run 1, which received energy from a grid mix, the following outcomes were obtained:

- The use of solar energy for Runs 1, 2, and 3 resulted in more than a 260% increase in the ADP element category. On the other hand, 58, 51, and 43% reductions in ADP elements were achieved when wind energy was used for Runs 1, 2, and 3, respectively. Therefore, the best outcome for ADP elements was reached for Run 1 by using wind as an energy source.
- For ADP fossil, using solar energy instead of grid electricity was observed to reduce the impact by 84 to 86% for all the runs. Usage of wind as the energy source rather than electricity lowered the ADP fossil by 95 to 97% for all treatment alternatives.
- Energy supply from solar panels was found to decrease AP by 81 to 84% for the runs. In the case of wind energy, reductions between 94 and 97% in AP were obtained for all the treatment conditions under investigation.
- In terms of EP, adopting solar energy resulted in 88–89% reductions, whereas obtaining energy from wind lowers this impact category by 97–98%.
- For FAETP, when using solar energy, 68–69% reductions were obtained for these runs. In the case of wind energy, FAETP was reduced by approximately 85% for all the experimental conditions.
- GWP was lowered by around 86% when solar energy was used for the runs. In comparison, 96% reductions in GWP were achieved by adopting wind as the energy source.

- Around 56–58% reductions were obtained for HTP when the energy source was shifted from grid electricity to solar energy. Moreover, for all the runs, HTP could be reduced by 87 to 89% when wind energy was used.
- Attaining energy from solar sources lowered MAETP by 76–77% for the runs. Furthermore, wind energy reduced MAETP by 95–96%.
- Using photovoltaic energy instead of grid electricity was found to increase ODP by 65, 78, and 92% for Runs 1, 2, and 3, respectively. In contrast, 75, 62, and 48% reductions in ODP could be obtained for Runs 1, 2, and 3, respectively, when the energy source is changed to wind.
- Values decreased by around 72 to 75% for POCP for all runs when solar energy was adopted. In contrast, the use of wind energy yielded over 91% reductions for Runs 1, 2, and 3.
- The use of photovoltaic cells instead of a grid mix lowered the TETP by more than 80% for all runs. Additionally, around 77 to 79% reductions were achieved when choosing wind energy.

One should note that all the presented results are based on laboratory data. Therefore, early research outcomes were evaluated in this study. There are a few pioneering LCA research activities that rely on lab data [15,46]. Such information can be used as a baseline for further appraisals of environmental impacts, especially for the adoption of full-scale activities [47–49]. Disparities are observed for the LCA results of the lab and upper-scale data [50]. Due to this fact, it is recommended that lab research studies be extended [50].

4. Conclusions

In the present work, the hydantoin fungicide and nematicide, iprodione, which was selected as the model micropollutant in this study, was subjected to photochemical treatment using UV-C-activated peroxydisulfate (PS) in synthetic, tertiary treated urban wastewater (TWW). It was aimed at examining the feasibility and sustainability of the proposed photochemical treatment system under kinetically optimized reaction conditions. The study revealed that a comprehensive treatability evaluation must cover both experimental (laboratory- and pilot-scale) research work as well as a detailed feasibility analysis to determine the environmental impacts of treatment alternatives or conditions with the aid of life cycle assessment (LCA). It was concluded that an integrated approach would yield more feasible, sustainable, and environmentally sound decisions regarding advanced oxidation applications.

The photochemical treatment combination provided several advantages over the use of UV-C only and PS only, both of which had only a minor (<10–15%) effect on iprodione removal from TWW. In addition, working under realistic conditions (with a real wastewater sample, a typical concentration of the target pollutant, etc.) could reduce the treatment efficiencies, but would be more meaningful when assessing the environmental impacts of the photochemical treatment method.

The energy input was quoted as the most important contributor to all investigated environmental impact categories. The study indicated that when the energy is obtained from grid electricity, the experimental run with 21.42 mg/L sodium peroxydisulfate and a 1.787 kWh/m³ energy requirement (Run 3) yielded the lowest unwanted environmental impacts for all of the investigated categories. In comparison with the conditions of Run 1 and obtaining energy from grid electricity, the following outcomes were revealed: In cases where the energy source is shifted to solar, elevated levels of ODP (by 65, 78, and 92% for Runs 1, 2, and 3, respectively) and ADP elements (by more than 260% for all the runs) were found. In contrast to this finding, when the energy was received from photovoltaic panels, reductions in AP, ADP fossil, EP, FAETP, GWP, HTP, MAETP, POCP, and TETP by more than 81, 84, 88, 67, 86, 56, 76, 72, and 80% were achieved, respectively. Wind energy was found to lower AP, ADP fossil, EP, FAETP, GWP, HTP, MAETP, POCP, and TETP by over 94, 95, 97, 85, 96, 87, 05, 91, and 77% for all experimental runs, respectively. Moreover, 58, 51, and 43% reductions for Runs 1, 2, and 3, respectively, were achieved for ADP elements

in the case of using wind energy. Additionally, lowering the ODP of Runs 1, 2, and 3 by 75, 62, and 48%, respectively, was accomplished when energy was obtained from wind instead of an electricity mix.

Finally, it should be emphasized that a complete evaluation of treatability must cover both experimental research and a sustainability assessment. Such an integrated approach will yield technically as well as environmentally sound decisions. In this respect, it is recommended to examine the environmental impacts of the treatability outcomes using an objective methodology such as the LCA before defining a treatment roadmap. With the information gathered from such an LCA study, decision-makers can prioritize the unwanted environmental impacts according to the specifications of the geographical area where they are working. Furthermore, upscaling LCA results based on laboratory data to industrial-scale or full-scale should be handled carefully.

Author Contributions: Conceptualization, F.G.B., B.A.T. and I.A.-A.; methodology, F.G.B., B.A.T. and I.A.-A.; software, B.A.T. and K.D.; validation, B.A.T. and K.D.; formal analysis, F.G.B., B.A.T. and I.A.-A.; investigation, F.G.B., B.A.T., I.A.-A. and K.D.; resources, F.G.B., B.A.T. and I.A.-A.; data curation, F.G.B., B.A.T., I.A.-A. and K.D.; writing—original draft preparation, F.G.B., B.A.T. and I.A.-A.; writing—review and editing, F.G.B., B.A.T., I.A.-A. and K.D.; visualization, F.G.B., B.A.T., I.A.-A. and K.D.; supervision, F.G.B., B.A.T. and I.A.-A.; project administration, F.G.B., B.A.T. and I.A.-A.; funding acquisition, F.G.B., B.A.T. and I.A.-A. All authors have read and agreed to the published version of the manuscript.

Funding: This research received no external funding.

Data Availability Statement: Data are contained within the article.

Acknowledgments: The authors thank Eksoy Chemicals (Turkey) for the reactive dye sample.

Conflicts of Interest: The authors declare no conflicts of interest. The funders had no role in the design of the study, in the collection, analysis, or interpretation of data, in the writing of the manuscript, or in the decision to publish the results.

References

1. Alvarino, T.; Lema, J.; Omil, F.; Suárez, S. Trends in organic micropollutants removal in secondary treatment of sewage. *Rev. Environ. Sci. Bio/Technol.* **2018**, *17*, 447–469. [\[CrossRef\]](#)
2. Edefell, E.; Falås, P.; Torresi, E.; Hagman, M.; Cimbritz, M.; Bester, K.; Christensson, M. Promoting the degradation of organic micropollutants in tertiary moving bed biofilm reactors by controlling growth and redox conditions. *J. Hazard. Mater.* **2021**, *414*, 125535. [\[CrossRef\]](#) [\[PubMed\]](#)
3. Falås, P.; Wick, A.; Castronovo, S.; Habermacher, J.; Ternes, T.A.; Joss, A. Tracing the limits of organic micropollutant removal in biological wastewater treatment. *Water Res.* **2016**, *95*, 240–249. [\[CrossRef\]](#) [\[PubMed\]](#)
4. Göbel, A.; McArdell, C.S.; Joss, A.; Siegrist, H.; Giger, W. Fate of sulfonamides, macrolides, and trimethoprim in different wastewater treatment technologies. *Sci. Total Environ.* **2007**, *372*, 361–371. [\[CrossRef\]](#) [\[PubMed\]](#)
5. Sezginer, I.; Turkmen, B.A.; Germirli Babuna, F. Environmental impacts arising from the production of two surface coating formulations. *Clean Technol. Environ. Policy* **2022**, *24*, 1811–1822. [\[CrossRef\]](#)
6. Ozsahin, B.; Elginöz, N.; Germirli Babuna, F. Life cycle assessment of a wind farm in Turkey. *Environ. Sci. Pollut. Res.* **2022**, *29*, 71000–71013. [\[CrossRef\]](#)
7. Karacal, P.; Elginöz, N.; Germirli Babuna, F. Environmental burdens of cataphoresis process. *Desalination Water Treat.* **2019**, *172*, 301–308. [\[CrossRef\]](#)
8. Ozkan, E.; Elginöz, N.; Germirli Babuna, F. Life cycle assessment of a printed circuit board manufacturing plant in Turkey. *Environ. Sci. Pollut. Res.* **2018**, *25*, 26801–26808. [\[CrossRef\]](#)
9. Ozkan, E.; Bas, B.; Elginöz, N.; Germirli Babuna, F. Environmental sensitivity of printed circuit board manufacturing to Cu recycling rate, transportation and various energy sources. *Int. J. Glob. Warm.* **2020**, *20*, 237–248. [\[CrossRef\]](#)
10. Saad, A.; Elginöz, N.; Germirli Babuna, F.; Iskender, G. Life cycle assessment of a large water treatment plant in Turkey. *Environ. Sci. Pollut. Res.* **2019**, *26*, 14823–14834. [\[CrossRef\]](#)
11. Sahin Akkurt, H.; Elginöz, N.; Iskender, G.; Germirli Babuna, F. Environmental Burdens of a Large Water Treatment Plant: The Operational Phase. In Proceedings of the 17th International Conference on Environmental Science and Technology, CEST, Athens, Greece, 1–4 September 2021. [\[CrossRef\]](#)
12. Elginöz, N.; Alzaboot, M.; Germirli Babuna, F.; Iskender, G. Construction of a large water treatment plant: Appraisal of environmental hotspots. *Desalinat. Water Treat.* **2019**, *172*, 309–315. [\[CrossRef\]](#)

13. Başkurt, M.; Kocababuç, I.; Binici, E.; Dulekgurgen, E.; Özgün, K.; Taşlı, R. Life cycle assessment as a decision support tool in wastewater treatment plant design with renewable energy utilization. *Desalination Water Treat.* **2017**, *93*, 229–238. [CrossRef]
14. Yalamacılar, B.; Elginoz, N.; Germirli Babuna, F. Benchmarking industrial water purification systems with the aid of life cycle assessment. *Desalination Water Treat.* **2021**, *211*, 422–431. [CrossRef]
15. Dogan, K.; Turkmen, B.A.; Germirli Babuna, F.; Uzun, O.K.; Alaton, I.A. Merging treatability results and sustainability assessment: A segregated textile dyehouse effluent. *Int. J. Environ. Sci. Technol.* **2023**, *20*, 11165–11176. [CrossRef]
16. Hashmi, M.Z.; Wang, S.; Ahmed, Z. *Environmental Micropollutants*; Elsevier: Amsterdam, The Netherlands, 2022; p. 469.
17. Pohanish, R.P. (Ed.) I:0075. In *Sittig's Handbook of Pesticides and Agricultural Chemicals*, 2nd ed.; William Andrew Publishing: Oxford, UK, 2015; pp. 483–506.
18. Commission Implementing Regulation (EU) 2017/2091. EUR-Lex—32017R2091—EN. 2017. Available online: <https://eur-lex.europa.eu/legal-content/EN/TXT/?qid=1512655318141&uri=CELEX:32017R2091> (accessed on 18 August 2023).
19. Iprodione (Rovral) Residues No Longer Permitted in Wine Imported into the European Union. Exporter News. 2018. Available online: <https://www.wineaustralia.com/news/articles/iprodione-residues-european-union> (accessed on 18 August 2023).
20. Montazeri, B.; Koba-Uzun, O.; Arslan-Alaton, I.; Olmez-Hanci, T. Iprodione Removal by UV-Light-, Zero-Valent Iron- and Zero-Valent Aluminium-Activated Persulfate Oxidation Processes in Pure Water and Simulated Tertiary Treated Urban Wastewater. *Water* **2021**, *13*, 1679. [CrossRef]
21. Martin, C.; Vega, D.; Bastide, J.; Davet, P. Enhanced degradation of iprodione in soil after repeated treatments for controlling *Sclerotinia minor*. *Plant Soil* **1990**, *127*, 140–142. [CrossRef]
22. Morales, J.; Manso, J.A.; Cid, A.; Mejuto, J.C. Stability study of Iprodione in alkaline media in the presence of humic acids. *Chemosphere* **2013**, *92*, 1536–1541. [CrossRef] [PubMed]
23. Olmez-Hanci, T.; Arslan-Alaton, I.; Imren, C. Performance of the Persulfate/UV-C Process for the Treatment of Dimethyl Phthalate from Aquatic Environments. *Int. J. Environ. Geoinform.* **2018**, *5*, 189–196. [CrossRef]
24. Juni, F.; Bashir, M.J.K.; Jaffari, Z.H.; Sethupathi, S.; Wong, J.W.C.; Zhao, J. Recent advancements in the treatment of emerging contaminants using activated persulfate oxidation process. *Separations* **2023**, *10*, 154. [CrossRef]
25. Deng, Y.; Zhao, R. Advanced Oxidation Processes (AOPs) in Wastewater Treatment. *Curr. Pollut. Rep.* **2015**, *1*, 167–176. [CrossRef]
26. Acero, J.L.; Benítez, F.J.; Real, F.J.; Rodríguez, E. Degradation of selected emerging contaminants by UV-activated persulfate: Kinetics and influence of matrix constituents. *Sep. Purif. Technol.* **2018**, *201*, 41–50. [CrossRef]
27. Schwack, W.; Bourgeois, B. Fungicides and photochemistry: Iprodione, procymidone, vinclozolin 1. Photodehalogenation. *Z. Lebensm.-Unters. Forsch.* **1989**, *188*, 346–347. [CrossRef]
28. Lassalle, Y.; Jellouli, H.; Ballerini, L.; Souissi, Y.; Nicol, É.; Bourcier, S.; Bouchonnet, S. Ultraviolet-vis degradation of iprodione and estimation of the acute toxicity of its photodegradation products. *J. Chromatogr. A* **2014**, *1371*, 146–153. [CrossRef] [PubMed]
29. Lopez-Alvarez, B.; Villegas-Guzman, P.; Peñuela, G.A.; Torres-Palma, R.A. Degradation of a Toxic Mixture of the Pesticides Carbofuran and Iprodione by UV/H₂O₂: Evaluation of Parameters and Implications of the Degradation Pathways on the Synergistic Effects. *Water Air Soil Pollut.* **2016**, *227*, 215. [CrossRef]
30. Montazeri, B.; Uzun, O.K.; Arslan-Alaton, I.; Olmez-Hanci, T. UV-C-activated persulfate oxidation of a commercially important fungicide: Case study with iprodione in pure water and simulated tertiary treated urban wastewater. *Environ. Sci. Pollut. Res.* **2020**, *27*, 22169–22183. [CrossRef] [PubMed]
31. Sphera. *GaBi V7.3 Software and Database*; Sphera: Chicago, IL, USA, 2017.
32. Ecoinvent. *Ecoinvent Database v.3.1*; Swiss Centre for Life Cycle Inventories: St. Gallen, Switzerland, 2013.
33. Guinée, J.B.; Gorée, M.; Heijungs, R.; Huppes, G.; Kleijn, R.; Koning, A. *Life Cycle Assessment: An Operational Guide to the ISO Standards*; Ministry of Housing, Spatial Planning and Environment (VROM) and Centre of environmental Science (CML): Leiden, The Netherlands, 2001. Available online: <https://web.universiteitleiden.nl/cml/ssp/projects/lca2/> (accessed on 15 July 2023).
34. *ISO 14040*; Environmental Management—Life Cycle Assessment—Principles and Framework. ISO: Geneva, Switzerland, 2006.
35. *ISO 14044*; Environmental Management—Life Cycle Assessment—Requirements and Guidelines. ISO: Geneva, Switzerland, 2006.
36. TEIAS. Electricity Generation and Transmission Statistics of Turkey. 2019. Available online: <https://www.teias.gov.tr/turkiye-elektrik-uretim-iletim-istatistikleri> (accessed on 2 June 2021).
37. Yang, Y.; Pignatello, J.J.; Ma, J.; Mitch, W.A. Effect of matrix components on UV/H₂O₂ and UV/S₂O₈²⁻ advanced oxidation processes for trace organic degradation in reverse osmosis brines from municipal wastewater reuse facilities. *Water Res.* **2016**, *89*, 192–200. [CrossRef] [PubMed]
38. Arslan-Alaton, I.; Olmez-Hanci, T.; Ozturk, T. Effect of inorganic and organic solutes on zero-valent aluminum-activated hydrogen peroxide and persulfate oxidation of bisphenol A. *Environ. Sci. Pollut. Res.* **2018**, *25*, 34938–34949. [CrossRef] [PubMed]
39. Wang, F.; Wu, Y.; Gao, Y.; Li, H.; Chen, Z. Effect of humic acid, oxalate and phosphate on Fenton-like oxidation of microcystin-LR by nanoscale zero-valent iron. *Sep. Purif. Technol.* **2016**, *170*, 337–343. [CrossRef]
40. Wang, J.; Wang, S. Effect of inorganic anions on the performance of advanced oxidation processes for degradation of organic contaminants. *Chem. Eng. J.* **2021**, *411*, 128392. [CrossRef]
41. Belghit, A.; Merouani, S.; Hamdaoui, O.; Bouhelassa, M.; Al-Zahrani, S. The multiple role of inorganic and organic additives in the degradation of Reactive Green 12 by UV/chlorine advanced oxidation process. *Environ. Technol.* **2022**, *43*, 835–847. [CrossRef]

42. Riga, A.; Soutsas, K.; Ntampeglitis, K.; Karayannis, V.; Papapolymerou, G. Effect of system parameters and of inorganic salts on the decolorization and degradation of Procion H-EXL dyes. Comparison of H₂O₂/UV, Fenton, UV/Fenton, TiO₂/UV and TiO₂/UV/H₂O₂ processes. *Desalination* **2007**, *211*, 72–86. [[CrossRef](#)]
43. Han, M.; Mohseni, M. Influence of sulfate and the interactions of major organic and inorganic solutes on the formation of nitrite during VUV photolysis of nitrate-rich water. *J. Environ. Chem. Eng.* **2021**, *9*, 105756. [[CrossRef](#)]
44. Zhang, Y.; Zhang, J.; Xiao, Y.; Chang, V.W.C.; Lim, T.-T. Kinetic and mechanistic investigation of azathioprine degradation in water by UV, UV/H₂O₂ and UV/persulfate. *Chem. Eng. J.* **2016**, *302*, 526–534. [[CrossRef](#)]
45. Mukherjee, J.; Lodh, B.K.; Sharma, R.; Mahata, N.; Shah, M.P.; Mandal, S.; Ghanta, S.; Bhunia, B. Advanced oxidation process for the treatment of industrial wastewater: A review on strategies, mechanisms, bottlenecks and prospects. *Chemosphere* **2023**, *345*, 140473. [[CrossRef](#)] [[PubMed](#)]
46. Mainardis, M.; Buttazzoni, M.; Gievers, F.; Vance, C.; Magnolo, F.; Murphy, F.; Goi, D. Life cycle assessment of sewage sludge pretreatment for biogas production: From laboratory tests to full-scale applicability. *J. Clean. Prod.* **2021**, *322*, 129056. [[CrossRef](#)]
47. Piccinno, F.; Hischer, R.; Seeger, S.; Som, C. From laboratory to industrial scale: A scale-up framework for chemical processes in life cycle assessment studies. *J. Clean. Prod.* **2016**, *135*, 1085–1097. [[CrossRef](#)]
48. Sun, Y.; Bai, S.; Wang, X.; Ren, N.; You, S. Prospective Life Cycle Assessment for the Electrochemical Oxidation Wastewater Treatment Process: From Laboratory to Industrial Scale. *Environ. Sci. Technol.* **2023**, *57*, 1456–1466. [[CrossRef](#)] [[PubMed](#)]
49. Erakca, M.; Bautista, S.P.; Moghaddas, S.; Baumann, M.; Bauer, W.; Leuthner, L.; Weil, M. Closing gaps in LCA of lithium-ion batteries: LCA of lab-scale cell production with new primary data. *J. Clean. Prod.* **2023**, *384*, 135510. [[CrossRef](#)]
50. Elginöz, N.; Atasoy, M.; Finnveden, G.; Cetecioglu, Z. Ex-ante life cycle assessment of volatile fatty acid production from dairy wastewater. *J. Clean. Prod.* **2020**, *269*, 122267. [[CrossRef](#)]

Disclaimer/Publisher's Note: The statements, opinions and data contained in all publications are solely those of the individual author(s) and contributor(s) and not of MDPI and/or the editor(s). MDPI and/or the editor(s) disclaim responsibility for any injury to people or property resulting from any ideas, methods, instructions or products referred to in the content.